Transient structural variations alter gene expression and quantitative traits in *Schizosaccharomyces pombe*.

Authors

Daniel C. Jeffares[1,2], Clemency Jolly[1], Mimoza Hoti[1,2], Doug Speed[2], Charalampos Rallis[1,2,3], Christophe Dessimoz[1,4,5,6*], Jürg Bähler[1,2*], Fritz J. Sedlazeck[7*]

Affiliation:

1. Department of Genetics, Evolution and Environment, University College London, London WC1E 6BT, United Kingdom.
2. UCL Genetics Institute, University College London, London WC1E 6BT, United Kingdom.
3. Current address: School of Health, Sport and Biosciences, University of East London, London E15 4LZ, United Kingdom.
4. Department of Computer Science, University College London, London WC1E 6BT, United Kingdom.
5. Department of Ecology and Evolution & Center for Integrative Genomics, University of Lausanne, Biophore, 1015 Lausanne, Switzerland.
6. Swiss Institute of Bioinformatics, Biophore, 1015 Lausanne, Switzerland
7. Department of Computer Science, Johns Hopkins University, 21218 Baltimore, USA

* Correspondence should be addressed to C.D. (christophe.dessimoz@unil.ch), J.B. (j.bahler@ucl.ac.uk) or F.J.S. (fritz.sedlazeck@jhu.edu)

Abstract

The effects of structural variants on phenotypic diversity and evolution are poorly understood. We recently described genetic and phenotypic variation among fission yeast strains and showed that genome-wide association studies are informative in this model. Here we extend this work by systematically identifying structural variations and investigating their consequences. We establish a curated catalog of copy number variants (CNVs) and rearrangements, including inversions and translocations. We show that CNVs substantially contribute to quantitative traits such as cell shape, cell growth under diverse conditions, sugar utilization in winemaking and antibiotic resistance, whereas rearrangements are strongly associated with reproductive isolation but contribute less to quantitative traits. We find that CNVs frequently vary within clonal populations and are weakly tagged by SNPs, consistent with rapid turnover, and produce measurable effects on gene expression both within and outside the repeated regions. Collectively, these findings have broad implications for evolution and for our understanding of quantitative traits and complex human diseases.

Keywords: structural variants, yeast, copy number variants, reproductive isolation, quantitative genetics, next generation sequencing

Structural variations (SVs), such as deletions, duplications, insertions, inversions or translocations, affect organismal phenotypes and complex diseases[1-3]. SVs also influence reproductive isolation within populations of yeast species[4-6] as well as flies and mosquitoes[7,8]. We, and others have recently begun to develop the fission yeast *Schizosaccharomyces pombe* as a model for population genomics and quantitative trait analysis[4,5,9-11]. This model organism combines the advantages of a small, well-annotated haploid genome[12], abundant tools for genetic manipulation and high-throughput phenotyping[13], and considerable resources of genome-scale and gene-centric data[14-16].

One facet of diversity studies in this species has been the discovery and analysis of a small number of inversions and reciprocal translocations[4,5,11]. Given this evidence for SVs in this species, we recognized that a systematic survey of SVs would progress our understanding of their biological influence. Here, we build upon the recent availability of 161 fission yeast genomes[10], representing the known population of this species worldwide, to undertake such a survey. We show that rearrangements contribute towards reproductive isolation, while copy number variants (CNVs) alter gene expression levels, contribute significantly to quantitative traits, and are transient within clonal populations.

RESULTS

Genome- and population-wide detection of structural variations

To predict an initial set of SVs, we applied four inference software packages (Delly, Lumpy, Pindel and cn.MOPs)[17-20] to existing short-read data[10], using parameters optimized on simulated data (Methods). We then filtered these initial predictions, accepting SVs detected by at least two callers, to obtain 315 variant calls (141 deletions, 112 duplications, 26 inversions, 36 translocations). We release this pipeline as an open source tool called SURVIVOR (Methods). To ensure a high specificity, we further filtered the 315 variants by removing SV calls whose breakpoints overlapped with low complexity regions or previously annotated long terminal repeats (LTRs)[10]. Finally, we manually vetted all the remaining SVs by visual inspection of read alignments in multiple strains for all 315 candidates. This meticulous approach aimed to ensure a high quality call set, to mitigate against the high uncertainty associated with SV calling[18].

This curation produced a set of 113 SVs, comprising 23 deletions, 64 duplications, 11 inversions and 15 translocations **(Figure 1a)**. Reassuringly, when our variant calling methods were applied to an engineered knockout strain, we correctly identified the known deletions and called no false positives. Attempts to validate all rearrangements by PCR and BLAST searches of *de novo* assemblies positively verified 76% of the rearrangements, leaving only a few PCR-intractable variants unverified (Methods).

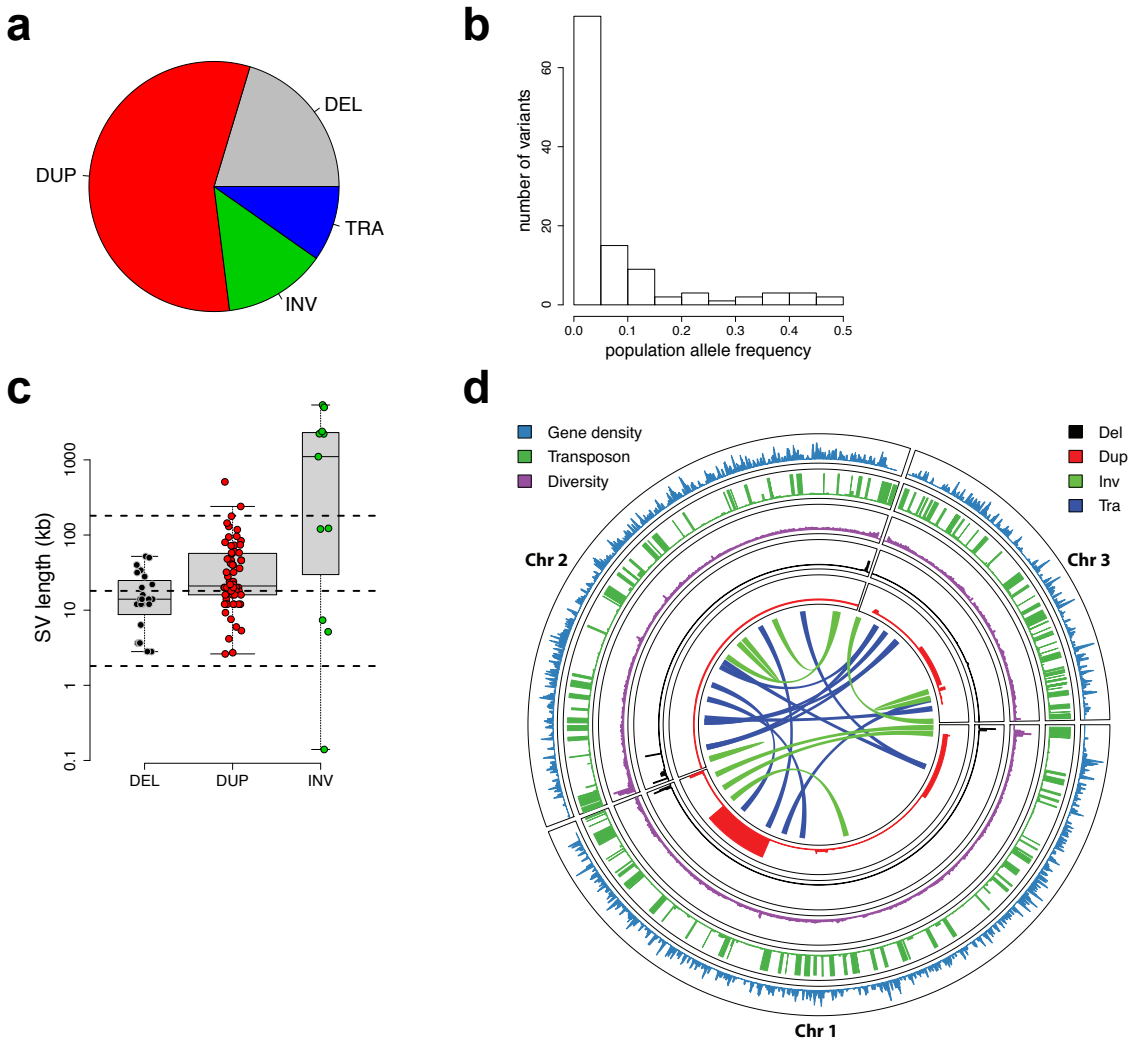

Figure 1. Characteristics of SVs in *S. pombe*. (**a**) Relative proportions of SVs identified. Duplications (DUP) were the most abundant SVs, followed by deletions (DEL), inversions (INV), and translocations (TRA). (**b**) Population allele frequency distribution of SVs, showing the frequencies of less abundant alleles in the population (minor allele frequencies). (**c**) Length distributions of SVs, $\log_{10}$ scale. Deletions were smallest (2.8–52 kb), duplications larger (2.6–510 kb), and inversions often very large, spanning large portions of chromosomes (1.04 kb–5,374 kb, see (d)). Horizontal dotted lines show the size of chromosome regions that contain an average of 1, 10 and 100 genes in this yeast. (**d**) Locations of SVs on the three chromosomes compared to other genomic features. From outside: density of essential genes, locations of *Tf*-type retrotransposons, diversity (π, average pairwise diversity from SNPs), deletions (black), duplications (red), and breakpoints of inversions and translocations as curved lines inside the concentric circles (green and blue, respectively). Bar heights for retrotransposons, deletions and

duplications are proportional to minor allele frequencies. Diversity and retrotransposon frequencies were calculated from 57 non-clonal strains as described by Jeffares, et al. [10].

Most SVs were present at low frequencies, with 28% discovered in only one of the strains analyzed **(Figure 1b)**. The deletions were generally small (median length 595bp, **Figure 1c)**, duplications showed a median length of 20 kb, with the largest duplication extending to 510 kb and covering 200 genes (a singleton in strain JB1207/NBRC10570). The majority of CNVs were present in copy numbers varying between zero and sixteen (subsequently we refer to amplifications of two or more copies as 'duplications').

Deletions and duplications and strongly biased towards the ends of chromosomes (**Figure 1d, Supplementary Figure 1**), which are characterized by high genetic diversity, frequent transposon insertions, and a paucity of essential genes[10]. All SVs preferentially occurred in positions of low gene density and showed a strong tendency to not overlap with essential genes (**Supplementary Figure 2**). To describe SVs further, we conducted gene enrichment analysis with the AnGeLi tool (**Supplementary Table 1**), which interrogates gene lists for functional enrichments using multiple qualitative and quantitative information sources[21]. The CNV-overlapping genes were enriched for caffeine/rapamycin induced genes and genes induced during meiosis ($P = 4x10^{-7}$ and $1x10^{-5}$, respectively); they also showed lower relative DNA polymerase II occupancy and were less likely to contain genes that are known to produce abnormal cell phenotypes ($P= 1.8x10^{-5}$ and $3x10^{-5}$, respectively). These analyses are all broadly consistent with a paucity of CNVs in genes that encode essential mitotic functions. Rearrangements disrupted only a few genes and showed no significant enrichments.

Duplications are transient within clonal populations

Our previous work identified 25 clusters of near-clonal strains, which differed by <150 SNPs within each cluster[10]. We expect that these clusters reflect either repeat depositions of strains differing only at few sites (e.g. mating-type variants of reference strains h^{90} and h^{-} differ by 14 SNPs) or natural populations of strains collected from the same location. Such 'clonal populations' reflect products of mitotic propagation from a very recent common ancestor, without any outbreeding. We therefore expected that SVs should be largely shared within these clonal populations.

Surprisingly, our genotype predictions indicated that most SVs present in clonal populations were segregating, i.e. were not fixed within the clonal population (68/95 SVs, 72%). Furthermore, we observed instances of the same SVs that were present in two or more different clonal populations, that were not fixed within any clonal population. These SVs could be either incorrect allele calls in some strains, or alternatively, recent events that have emerged during mitotic propagation. To distinguish between these two scenarios, we re-examined the read coverage of all 49 CNVs present within at least one

clonal population. Since translocations and inversions were more challenging to accurately genotype, we did not re-examine these variants. This analysis verified that 40 of these 49 CNVs (37 duplications, 3 deletions) were clearly segregating within at least one clonal cluster **(Figure 2a, Supplementary Figure 3)**. For example, one clonal population of seven closely related strains, collected together in 1966 from grape must in Sicily, have an average pairwise difference of only 19 SNPs (diversity $\pi = 1.5 \times 10^{-6}$). Notably, this collection showed four non-overlapping segregating duplications. This striking finding indicates that CNVs can arise or disappear frequently during evolution.

Transient duplications affect gene expression

Partial aneuploidies of 500-700 kb in the *S. pombe* reference strain are known to alter gene expression levels within and, to some extent, outside of the duplicated region[22]. The naturally occurring duplications we described are typically smaller (median length: 46 kb), including an average of 6.5 genes. To examine whether naturally occurring CNVs have similar effects on gene expression, we examined eight pairs of closely related strains (<150 SNPs among each pair) that contained at least one unshared duplication **(Figure 2b, Supplementary Figure 3, Supplementary Table 2)**. Several of these strain pairs have been isolated from the same substrate at the same time, and all pairs are estimated to have diverged approximately 50 to 65 years ago (**Supplementary Table 2**). We assayed transcript expression from log phase cultures using DNA microarrays, comparing duplicated to non-duplicated strains within the same clonal population. In seven of the eight strain pairs, the expression levels of genes within duplications were significantly induced, although the degree of expression changes between genes was variable **(Figure 2c)**. The increased transcript levels correlated with the increased genomic copy numbers, so that higher copy numbers produced correspondingly more transcripts (**Supplementary Figure 4**). No changes in gene expression were evident immediately adjacent to the duplications (**Supplementary Figure 4)**, suggesting that the local chromatin state was not strongly altered by the CNVs.

Some genes outside the duplicated regions also showed altered expression levels **(Figure 2d, Supplementary Table 3)**. For example, two strain pairs differ by a single 12 kb duplication. Here, five of seven genes within the duplication showed induced expression, while 45 genes outside the duplicated region also showed consistently altered expression levels (38 protein-coding genes, 7 non-coding RNAs) (**Figure 2d**, arrays 7 and 8). As environmental growth conditions were tightly controlled, these changes in gene expression probably reflect indirect and compensatory effects of the initial perturbation caused by the duplication (**Supplementary Figure 5**). We conclude that these evolutionary unstable duplications reproducibly affect the expression of distinct sets of genes and thus have the potential to influence cellular function and phenotypes.

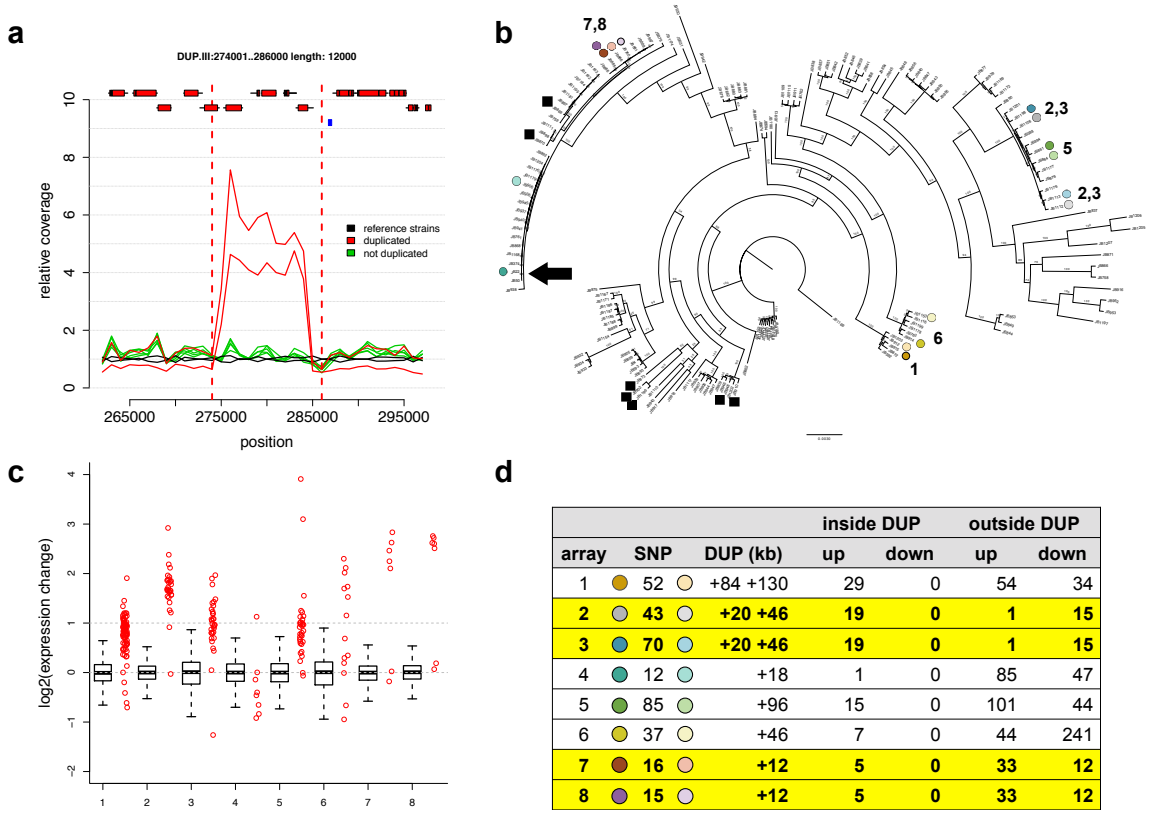

				inside DUP		outside DUP	
array		SNP	DUP (kb)	up	down	up	down
1		52	+84 +130	29	0	54	34
2		**43**	**+20 +46**	**19**	**0**	**1**	**15**
3		**70**	**+20 +46**	**19**	**0**	**1**	**15**
4		12	+18	1	0	85	47
5		85	+96	15	0	101	44
6		37	+46	7	0	44	241
7		**16**	**+12**	**5**	**0**	**33**	**12**
8		**15**	**+12**	**5**	**0**	**33**	**12**

Figure 2. Transient duplications affect gene expression. (**a**) Duplications occur within near-clonal strains. Plot showing average read coverage in 1 kb windows for two clonal strains (JB760, JB886) with the duplication (red), five strains without duplication (green), and two reference strains (h^+, and h-) (black). Genes (with exons as red rectangles) and retrotransposon LTRs (blue rectangles) are shown on top. See **Supplementary Table 2** for details. (**b**) Eight pairs of closely related strains, differing by one or more large duplications, selected for expression analysis. The tree indicates the relatedness of these strain pairs (dots colored as in d). The position of the reference strain (Leupold's 972, JB22) is indicated with a black arrow. Black squares indicate the presence of a 32 kb duplication that is associated with Brefeldin resistance (see below). (**c**) Gene expression increases for most genes within duplicated regions. For each tested strain pair, we show gene expression for all genes outside the duplication (as boxplot) and for all genes within the duplication (red strip chart). In all but one case (array 4), the genes within the duplication tend to be more highly expressed than the genes outside of the duplication (all Wilcoxon rank sum test P-values $<1.5\times10^{-3}$). (**d**) Summary of expression arrays 1-8, with strains indicated as colored dots (as in b), showing number of single-nucleotide polymorphism differences between strains (SNP), sizes of duplications in kb (DUP, where '+X +Y' indicates two duplications with length X and length Y, respectively). We show total numbers of induced (up) and repressed (down) genes, both inside and outside

the duplicated regions. Arrays 2,3 and 7,8 (in yellow shading) are replicates within the same clonal population that contain the same duplications, so we list the number of up- and down-regulated genes that are consistent between both arrays. See **Supplementary Tables 3 and 4** for details.

Copy number variants influence quantitative traits

To test whether SVs affect phenotypes, we examined the contributions of SNPs, CNVs and rearrangements to 53 quantitative traits, including 11 cell shape parameters and colony size on solid media assaying 42 stress and nutrient conditions[10]. For each phenotype, we used mixed model analysis to estimate the total proportion of variance explained by the additive contribution of genomic variants (the narrow-sense heritability). When we determined heritability using only SNP data, estimates varied between 0% and 74%.

When we used SNPs, CNVs and rearrangements in a composite model, the estimated overall heritability increased for nearly all traits, in some cases by more than 2-fold (e.g., resistance to Rapamycin) (**Fig 3a**). This finding indicates that the CNVs and rearrangements can explain a substantial proportion of the trait variance. Using this composite model, we quantified the individual contributions of heritability best explained by SNPs, CNVs and rearrangements (**Fig 3b**). On average, SNPs explained 30% of trait variance, CNVs 14%, and rearrangements 5% (**Supplementary Figure 6, Supplementary Table 5**). Analysis of simulated data confirmed that the contribution of CNVs could not be explained by linkage to causal SNPs alone (**Supplementary Figure 6**).

As some of the strains have recently been shown to be fermentation properties that may be beneficial for winmaking[46], we examined three traits related to wine fermentations (glucose/fructose utilization, malic acid degradation, acetic acid content). Remarkably, the heritability of these wine-fermentation traits was almost entirely due to SVs, with negligible contributions from SNPs (**Supplementary Figure 7, Supplementary Table 6**). For glucose/fructose utilization, the CNVs accounted for the entire heritability of 0.53 (**Supplementary Figure 8**). Since many of these strains have been collected from fermentations (**Supplementary Table 7**), the strong influence of CNVs may represent recent strong selection and adaptation to fermentation conditions, that has occurred via recent CNV acquisition.

To locate specific SVs that affected these traits, we performed mixed model genome-wide association studies, using all 68 SVs with minor allele counts >5 as well as 139,396 SNPs and 22,058 indels. Trait-specific significance thresholds for 5% familywise error rates were computed via permutation analysis, and were approximately 10^{-4} (SVs), 10^{-6} (SNPs and indels). Five SVs were significantly associated with traits (3 duplications, 1 deletion, 1 translocation) (**Supplementary Table 8**). The median effect

size was 9% (range 6-13%). The strongest signal was from a 32kb duplication that affected 11 protein-coding genes, which was significantly associated with 15 growth traits. This duplication is segregating (not fixed) within three clonal populations (**Fig. 2b, Supplementary Figure 9**), often as part of a larger duplication. It was the most significantly associated variant (from SNPs, indels and SVs) for growth in the antibiotic Brefeldin, where it contributes 15% of the trait variance (**Supplementary Figure 10**). Three of the 11 duplicated genes encode transmembrane proteins, any of which could contribute to the trait. Since fungi produce Brefeldin to inhibit competitive growth, this duplication is a striking example of a transient CNV that could provide a strong selective advantage.

Our analysis of heritability showed that SNPs are able to broadly predict most of the genetic contribution of SVs (**Fig. 3**). To examine whether trait-influencing SVs will be effectively detected by tagging SNPs in in this population, we examined the linkage of all 113 SVs with SNPs. We found that only 63 of these SVs (55%) are in strong linkage (r^2 >0.6), leaving 45% of the SVs weakly linked (**Supplementary Table 16**). This lack of linkage is consistent with SVs being transient, rather than persisting within haplotypes. Collectively, these analyses indicate that SVs, most notably CNVs, contribute substantially to quantitative traits and suggests that GWAS analyses conducted without genotyping SVs could fail to capture these genetic factors.

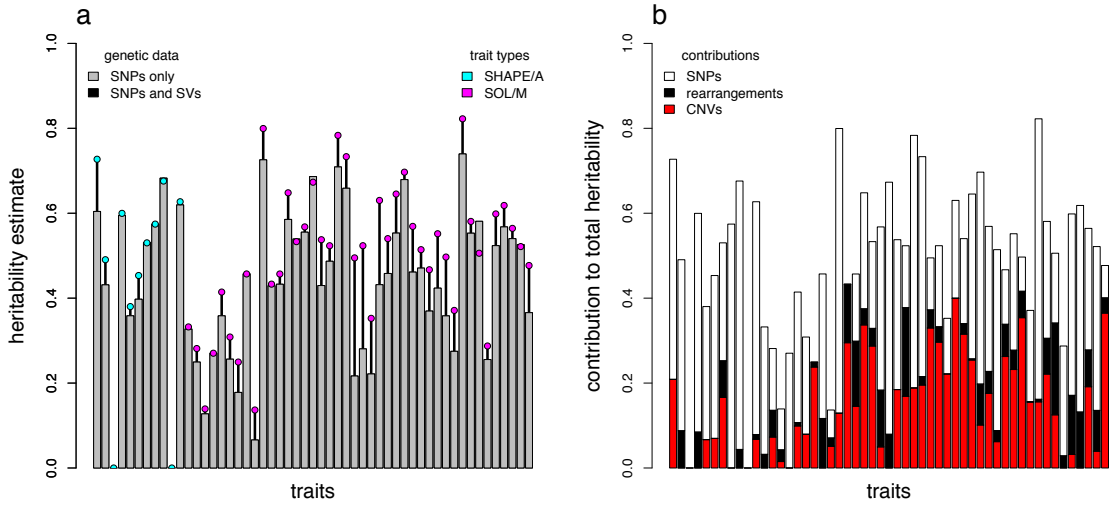

Figure 3. CNVs contribute to quantitative traits. (**a**) Heritability estimates obtained using SNPs alone (grey bars) are generally lower than estimates obtained using SNPs, CNVs and rearrangements (black lines extending above bars), consistent with CNVs and rearrangements contributing to traits. The types of traits described are indicated by the filled circles, including automated shape parameters (SHAPE/A), and growth rates on solid media (SOL/M). (**b**) Contributions of CNVs (red), rearrangements (black) and SNPs (open bars) to total heritability are shown with a stacked bar plot. CNVs in

particular make substantial contributions that will be associated with non-causal SNPs in cases when the causal CNVs have not been included in the genetic data.

Structural variations contribute to intrinsic reproductive isolation

Crosses between *S. pombe* strains produce between 90% and < 1% viable offspring[4,11]. We have previously shown that spore viability correlates inversely with the number of SNPs between the parental strains[10]. This intrinsic reproductive isolation may be due to the accumulation of Dobzhansky-Muller incompatibilities (variants that are neutral in one population, but incompatible when combined)[23,24]. However, genetically distant strains also accumulate SVs, which are known to lower hybrid viability and drive reproductive isolation[6]. In *S. pombe,* engineered inversions and translocations reduce spore viability by ~40%[4].

To analyse intrinsic reproductive isolation in more detail, we examined the relationship between viability, SNPs and SVs. Both SV-distance (number of unshared SVs between parents) and SNP-distance inversely correlated with hybrid viability (Kendall correlation coefficients, SVs: $\tau = -0.26$, $P = 5.6 \times 10^{-3}$, SNPs: $\tau = -0.35$, $P = 1.6 \times 10^{-4}$) (**Supplementary Figure 11**). While inversions and translocations are known to lower hybrid viability as they affect chromosome pairing and segregation during meiosis[4,11,25], CNVs are not expected to influence spore viability. Consistent with this view, we found that rearrangements explained spore viability better than CNVs (rearrangements, $\tau = -0.36$, $P = 2.0 \times 10^{-4}$; CNVs, $\tau = -0.10$, $P = 0.28$).

As the numbers of SNP and rearrangement differences between mating parents are themselves correlated ($\tau = 0.53$, $P = 1.3 \times 10^{-8}$), we also estimated the influence of each factor alone using partial correlations. When either SNPs or rearrangements were controlled for, both remained significantly correlated with offspring viability ($P = 0.04$, $P = 0.02$, respectively) (**Figure 4**). Taken together, these analyses indicate that both rearrangements and SNPs contribute to reproductive isolation, but CNVs do not.

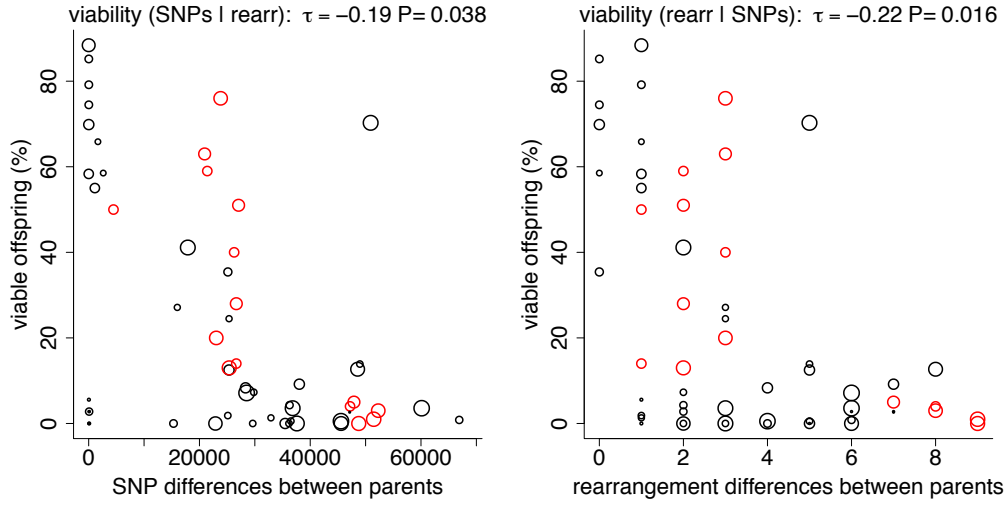

Figure 4. Both SNPs and rearrangements contribute to intrinsic reproductive isolation. Spore viability was measured from 58 different crosses from Jeffares, et al. [10] (black) or Avelar, et al. [4] (red), with each circle in the plots representing one cross. An additive linear model incorporating both SNP and rearrangement differences showed highly significant correlations with viability ($P = 1.2x10^{-6}$, $r^2 = 0.39$). Both genetic distances measured using SNPs and rearrangements (inversions and translocations) significantly correlated with viability when controlling for the other factor (Kendall partial rank order correlations with viability SNPs|rearrangements $\tau = -0.20$, $P = 0.03$; rearrangements|SNPs $\tau = -0.22$, $P = 0.02$). Some strains produce low viability spores even when self-mated with their own genotype. The lowest self-mating viability of each strain pair is indicated by circle size (smaller circles indicate lower self-mating viability) to illustrate that low-viability outliers tend to include such cases (see **Supplementary Table 9** for details).

DISCUSSION

Here we present the first genome- and population-wide catalog of SVs among *S. pombe* strains. To account for the high discrepancy of available methods[18], we applied a consensus approach to identify SVs (SURVIVOR), followed by rigorous filtering and manual inspection of all calls. We focused on high specificity (the correctness of the inferred SV) rather than high sensitivity (attempting to detect all SVs).

Our previous analyses[10], conducted without SV data, attributed both trait variations and reproductive isolation to SNPs and/or small indels. Here we show that the small number of SVs we describe make substantial contributions to both of these factors. We demonstrate that CNVs (duplications and deletions) contribute significantly to our ability to describe quantitative traits, whereas variants that rearrange the order of the genome (inversions and translocations) produce much weaker effects on traits. In contrast, CNVs have no detectable influence on reproductive isolation, while rearrangements contribute substantially to reproductive isolation, similar to other species[7,26].

A surprising aspect of our analysis is that duplications are generated and/or lost frequently within clonal populations. For example, within seven strains that differ by as few as 19 SNPs, we discovered four segregating duplications. A similar rapid occurrence of duplications in *S. pombe* has been observed in laboratory conditions, where spontaneous duplications suppress *cdc2* mutants at least 100 times more frequently than SNPs, and these suppressor strains lose their duplications with equal frequency[27]. Similarly, duplications frequently occur during experimental evolution with budding yeast[28]. Consistent with the transience of these variants, they are frequently not well tagged by SNPs. These CNVs subtly alter the expression of genes within and beyond the duplications, and contribute considerably to quantitative traits. Within small populations,

CNVs may produce larger effects on traits in the short term than SNPs, as demonstrated by the 32 kb duplication that is associated with resistance to the Brefeldin A (an antibiotic produced by entophytic fungi).

This analysis has relevance for human diseases, since *de novo* CNV formation in the human genome occurs at a measurable rate (approximately one CNV/10 generations[29]), and CNVs are known to contribute to a wide variety of diseases[30]. Indeed, both the population genetics and the effects of SVs within *S. pombe* seem similar to human, in that CNVs have been shown to be associated with stoichiometric changes on gene expression[31], and the recent population survey of SVs in the human genome has shown that SVs are frequently not in strong linkage to SNPs[32].

In summary, we show that a small number of SVs produce profound effects on the biology of this species. Different types of SVs have distinct influences at the phenotype level. Our findings highlight the need to identify SVs when describing traits using GWAS, and indicate that the contribution of SNPs to traits will often be overestimated when SVs are not typed.

METHODS

Performance assessment of SV callers using simulated data

To identify filtering parameters for DELLY, LUMPY and Pindel for the *S. pombe* genome, we simulated seven datasets (s1-s7) of 40x coverage with a range of different SV types and sizes (**Supplemental Table 7**). The simulated read sets contained sequencing errors (0.4%), SNPs and indels (0.1%) within the range of actual data from *S. pombe* strains and between 30 and 170 SVs. These data sets were produced by modifying the reference genome using our in-house software (SURVIVOR, described below), and simulating reads from this genome with Mason software[33].

After mapping the reads and calling SVs, we evaluated the calls. We defined a SV correctly predicted if: i) the simulated and reported SV were of the same type (e.g. duplication), ii) were predicted to be on same chromosome, and iii) their start and stop locations were with 1 kb. We then defined caller-specific thresholds to optimize the sensitivity and false discovery rate (FDR) for each caller. FDRs on the simulated data were low: DELLY (average 0.13), LUMPY (average 0.06) and Pindel (average 0.04).

Selecting calls that were present in at least two callers further reduced the FDR (average of 0.01). DELLY had the highest sensitivity (average 0.75), followed by SURVIVOR (average 0.70), LUMPY (average 0.62) and Pindel (0.55). We further used simulated data to assess the sensitivity and FDR of our predictions. cn.mops was evaluated with a 2 kb distance for start and stop coordinates. Our cn.mops parameters were designed to identify large (above 12 kb) events and thus did not identify any SVs simulated for s1-s6. Details of simulations and caller efficacy are provided in **Supplementary Table 10**.

SURVIVOR (StructURal Variant majorIty VOte) Software Tool

We developed the SURVIVOR tool kit for assessing SVs for short read data that contains several modules. The first module simulates SVs given a reference genome file (fasta) and the number and size ranges for each SV (insertions, deletions, duplications, inversions and translocations). After reading in the reference genome, SURVIVOR randomly selects the locations and size of SV following the provided parameters. Subsequently, SURVIVOR alters the reference genome accordingly and prints the so altered genome. In addition, SURVIVOR provides an extended bed file to report the locations of the simulated SVs.

The second module evaluates SV calls based on a variant call format (VCF) file [34] and any known list of SVs. A SV was identified as correct if i) they were of same type (e.g. deletion); ii) they were reported on same chromosome, and iii) the start and stop coordinates of the simulated and identified SV were within 1 kb (user definable).

The third module of SURVIVOR was used to filter and combine the calls from three VCF files. In our case, these files were the results of DELLY, LUMPY and Pindel. This module includes methods to convert the method-specific output formats to a VCF

format. SVs were filtered out if they were unique to one of the three VCF files. Two SVs were defined as overlapping if they occur on the same chromosome, their start and stop coordinates were within 1 kb, and they were of the same type. In the end, SURVIVOR produced one VCF file containing the so filtered calls. SURVIVOR is available at github.com/fritzsedlazeck/SURVIVOR.

Read mapping and detection of structural variants

Illumina paired-end sequencing data for 161 *S. pombe* strains were collected as described in Jeffares, et al. [10], with the addition of Leupold's reference 975 h^+ (JB32) and excluding JB374 (known to be a gene-knockout version of the reference strain, see below). Leupold's 968 h^{90} and Leupold's 972 h^- were included as JB50 and JB22, respectively (**Supplementary Table 7**). For all strains, reads were mapped using NextGenMap (version 0.4.12)[35] with the following parameter (-X 1000000) to the *S. pombe* reference genome (version ASM294v2.22). Reads with 20 base pairs or more clipped were extracted using the script *split_unmapped_to_fasta.pl* included in the LUMPY package (version 0.2.9)[18] and were then mapped using YAHA (version 0.1.83)[36] to generate split-read alignments. The two mapped files were merged using Picard-tools (version 1.105) (http://broadinstitute.github.io/picard), and all strains were then down-sampled to 40x coverage using Samtools (version 0.1.18)[37].

Subsequently, DELLY (version 0.5.9, parameters: " –q 20 -r")[19], LUMPY (version 0.2.9, recommended parameter settings)[18] and Pindel (version 0.2.5a8, default parameter)[20] were used to independently identify SVs in the 161 strains using our SURVIVOR software. We then retained all variants predicted by at least two methods. These SVs calls were genotyped using DELLY.

To identify further CNVs, we ran cn.MOPS[17] with parameters tuned to collect large duplications/deletions as follows: read counts were collected from bam alignment files (as above) with *getReadCountsFromBAM* and WL=2000, and CNVs predicted using *haplocn.mops* with minWidth= 6, all other parameters as default. Hence, the minimum variant size detected was 12 kb. CNV were predicted for each strain independently by comparing the alternative strain to the two reference strains (JB22, JB32) and four reference-like strains that differed from the reference by less than 200 SNPs (JB1179, JB1168, JB937, JB936).

After CNV calling, allele calling was achieved by comparing counts of coverage in 100bp windows for the two reference strains (JB22, JB32) to each alternate strain using custom R scripts. Alleles were called as non-reference duplications if the one-sided Wilcoxon rank sum test p-values for both JB22 and JB32 vs alternate strain were less than $1x10^{-10}$ (showing a difference in coverage) and the ratio of alternate/reference coverage (for both JB22 and JB32) was >1.8 (duplications), or <0.2 (deletions). Manual inspection of coverage plots showed that the vast majority of the allele calls were in accordance with what we discerned by eye. These R scripts were also used to examine

CNVs predicted to be segregating within clusters (clonal populations). All such CNVs were examined in all clusters that contained at least one non-reference allele call (**Supplementary Table 11**).

Finally, we manually mapped two large duplications that did not satisfy these criteria (DUP.I:2950001..3190000, 240kb and DUP.I:5050001..5560000, 510kb – both singletons in JB1207), but were clearly visible in chromosome-scale read coverage plots **(Supplementary Figure 12).**

Reduction of false discovery rate

This filtering produced 315 variant calls. However, because 31 of these 315 (~10%) were called within the two reference strains (JB22, JB32), we expected that this set still contained false positives. To further reduce the false positive rate, we looked for parameters that would reduce calls made in reference strains (JB22 and JB32) but not reduce calls in strains more distantly related to the reference (JB1177, JB916 and JB894 that have 68223, 60087 and 67860 SNP differences to reference[10]). The reasoning was that we expected to locate few variants in the reference, and more variants in the more distantly related strains. This analysis showed that paired end support, repeats and mapping quality were of primary value.

We therefore discarded all SVs that had a paired end support of 10 or less. In addition, we ignored SVs that appeared in low mapping quality regions (i.e. regions where reads with MQ=0 map) or overlapped with previously identified retrotransposon LTRs[10].

Finally, to ensure a high specificity call set, these filtered SVs were manually curated using IGV[38] (**Supplementary Tables 12,13**). We assigned each SVs a score (0: not reliable, 1: unclear, 2: reliable based on inspection of alignments through IGV). Only calls passing this manual curation as reliable (score 2) were included in the final data set of 113 variants utilized for all further analyses.

These filtering and manual curation steps reduced our variant calls substantially, from 315 to 113. At this stage only 1/113 (~1%) of these variants was called within the two reference strains (JB22, JB32).

PCR validation

PCR analysis was performed to confirm 10 of the 11 inversions and all 15 translocations from the curated data set. One inversion was too small to examine by PCR (INV.AB325691:6644..6784, 140 nt). Primers were designed using Primer3[39] to amplify both the reference and alternate alleles. PCR was carried out with each primer set using a selection of strains that our genotype calls predict to include at least one alternate allele and at least one reference allele (usually 6 strains). Products were scored according to product size and presence/absence (**Supplementary Tables 14, 15**).

Inversions: 9/10 variants were at least partially verified by either reference or alternate allele PCR (3 variants were verified by both reference and alternate PCRs), and 7/10 inversions also received support from BLAST (see below). Translocations: 10/15 were at least partially verified by either reference or alternate allele PCR (5/15 variants were verified by both reference and alternate PCRs). One additional translocation received support from BLAST (see below), meaning that 11/15 translocations were supported by PCR and/or BLAST. Three of the four translocations that could not be verified were probably nuclear copies of mitochondrial genes (NUMTs)[40], because one breakpoint was mapped to the mitochondrial genome.

Validation by BLAST of *de novo* assemblies

We further assessed the quality of the predicted breakpoints for the inversions and translocations by comparing them to the previously created *de novo* assemblies for each of the 161 strains[10].To this end, we created blast databases for the scaffolds of each strain that were >1kb. We then created the predicted sequence for 1 kb around each junction of the validated 10 inversions and 15 translocations. These sequences were used to search the blast databases using BLAST+ with --gapopen 1 --gapextend 1 parameters. We accepted any blast hsp with a length >800 bp as supporting the junction (because these must contain at least 300 bp at each side of the break point). Four inversions and three translocations gained support from these searches (Supplementary File Tables2-PCR.xlsx).

Knockout strain control

Our sample of sequenced strains included one strain (JB374) that is known to contain deletions of the *his3* and *ura4* genes. Our variant calling and validation methods identified only two variants in this strain, both deletions that corresponded to the positions of these genes, as below:

his3 gene location is chromosome II, 1489773-1488036, deletion detected at II:1488228-1489646.

ura4 gene location is chromosome III, 115589-116726, deletion detected at III:115342-117145.

This strain was not included in the further analyses of the SVs.

Microarray expression analysis

Cells were grown in YES (Formedium, UK) and harvested at OD_{600} =0,5. RNA was isolated followed by cDNA labeling[41]. Agilent 8 x 15K custom-made *S. pombe* expression microarrays were used. Hybridization, normalization and subsequent washes were performed according to the manufacturer's protocols. The obtained data were scanned and extracted using GenePix and processed for quality control and normalization using in-house developed R scripts. Subsequent analysis of normalized data was

performed using R. Microarray data have been submitted to ArrayExpress (accession number E-MTAB-4019). Genes were considered as induced if their expression signal after normalization was >1.9, and repressed if <0.51.

Time to most recent common ancestor (TMRCA) estimates

Previously, based on the genetic distances between these strains and the 'dated tip' dating method implemented in BEAST[42], we have estimated the divergence times between all 161 *S. pombe* strains sequenced[10]. To determine the TMRCA for pairs of strains, we re-examined the BEAST outputs using FigTree to obtain the medium and 95% confidence intervals.

SNP and indel calling

SNPs were called as described[10]. Insertions and deletions (indels) were called in 160 strains using stampy-mapped, indel-realigned bams as described previously[10]. We accepted indels that were called by both the Genome Analysis Toolkit HaplotypeCaller[43] and Freebayes[44], and then genotyped all these calls with Freebayes.

Briefly, indels were called on each strains bam with HaplotypeCaller, and filtered for call quality >30 and mapping quality >30 (bcftools filter --include 'QUAL>30 && MQ>30'). Separately, indels were called on each strains bam with Freebayes, and filtered for call quality >30. All Freebayes vcf files were merged, accepting only positions called by both Freebayes and HaplotypeCaller. These indels were then genotyped with Freebayes using a merged bam (containing reads from all strains), using the --variant-input flag for Freebayes to genotyped only the union calls. Finally indels were filtered for by score, mean reference mapping quality and mean alternate mapping quality >30 (bcftools filter --include 'QUAL>30 && MQM>30 & MQMR>30'). These methods identified 32,268 indels. Only 50 of these segregated between Leupold's h^- reference (JB22) and Leupold's h^{90} reference (JB50), whereas 12109 indels segregated between the JB22 reference and the divergent strain JB916.

Heredity and GWAS

We selected 53 traits that contained at least values from 100 strains[10], and so included multiple individuals from within clonal populations (growth rates on 42 different solid media and 11 cell shape characters measured with automated image analysis). Trait values were normalized using a rank-based transformation in R, for each trait vector y, normal.y =qnorm(rank(y)/(1+length(y))). Total heritability, and the contribution of SNPs, CNVs and rearrangements were estimated using LDAK (version 5.94)[45], with kinship matrices derived from all SNPs, 87 CNVs, and 26 rearrangements. To assess whether the contribution of CNVs could be primarily due to linkage with causal SNPs, we simulated trait data using the --make-phenos function of LDAK with the relatedness matrix from all SNPs, assuming that all variants contributed to the trait (--num-causals -1). We made one

simulated trait data set per trait, for each of the 53 traits, with total heritability defined as predicted from the real data. We then estimated the heritability using LDAK, including the joint matrix of SNPs, CNVs and rearrangements. To assess the extent to which the contribution of SNPs to heritability was overestimated, we performed another simulation using the relatedness matrix from the 87 segregating CNVs alone, and then estimated the contribution of SNPs, CNVs and rearrangements in this simulated data as above.

Genome-wide associations were performed with LDAK (version 5) using default parameters, using a mixed model derived from kinship of all SNPs called previouslyJeffares, et al. [10]. Association analysis was run separately for 68 SVs with a minor allele count >5, for 139,396 SNPs and for 22,058 indels, both minor allele counts >5. We examined the same 53 traits as for the heritability analysis (above). For each trait, we carried out 1000 permutations of trait data, and define the 5th percentile of these permutations as the trait-specific P-value threshold.

Offspring viability and genetic distance

Cross spore viability data and self-mating viability were collected from previous analyses[4,10]. The number of differences between each pair was calculated using vcftools vcf-subset[34], and correlations were estimated using R, with the ppcor package. When calculating the number of CNVs differences between strains, we altered our criteria for 'different' variants (to merge variants whose starts and ends where within 1 kb), and merged CNVs if their overlap was >50% and their allele calls were the same.

References

1. Klopocki, E. & Mundlos, S. Copy-number variations, noncoding sequences, and human phenotypes. *Annu Rev Genomics Hum Genet* **12**, 53-72 (2011).
2. Stefansson, H. *et al*. CNVs conferring risk of autism or schizophrenia affect cognition in controls. *Nature* **505**, 361-6 (2014).
3. Walters, R.G. *et al*. Rare genomic structural variants in complex disease: lessons from the replication of associations with obesity. *PLoS One* **8**, e58048 (2013).
4. Avelar, A.T., Perfeito, L., Gordo, I. & Ferreira, M.G. Genome architecture is a selectable trait that can be maintained by antagonistic pleiotropy. *Nat Commun* **4**, 2235 (2013).
5. Brown, W.R. *et al*. A Geographically Diverse Collection of Schizosaccharomyces pombe Isolates Shows Limited Phenotypic Variation but Extensive Karyotypic Diversity. *G3 (Bethesda)* **1**, 615-26 (2011).
6. Rieseberg, L.H. Chromosomal rearrangements and speciation. *Trends Ecol Evol* **16**, 351-358 (2001).
7. Ayala, D., Guerrero, R.F. & Kirkpatrick, M. Reproductive isolation and local adaptation quantified for a chromosome inversion in a malaria mosquito. *Evolution* **67**, 946-58 (2013).
8. McGaugh, S.E. & Noor, M.A. Genomic impacts of chromosomal inversions in parapatric Drosophila species. *Philos Trans R Soc Lond B Biol Sci* **367**, 422-9 (2012).
9. Fawcett, J.A. *et al*. Population genomics of the fission yeast Schizosaccharomyces pombe. *PLoS One* **9**, e104241 (2014).
10. Jeffares, D.C. *et al*. The genomic and phenotypic diversity of Schizosaccharomyces pombe. *Nat Genet* **47**, 235-41 (2015).
11. Zanders, S.E. *et al*. Genome rearrangements and pervasive meiotic drive cause hybrid infertility in fission yeast. *Elife* **3**, e02630 (2014).
12. Wood, V. *et al*. The genome sequence of Schizosaccharomyces pombe. *Nature* **415**, 871-80 (2002).
13. Sabatinos, S.A. & Forsburg, S.L. Molecular genetics of Schizosaccharomyces pombe. *Methods Enzymol* **470**, 759-95 (2010).
14. Kim, D.U. *et al*. Analysis of a genome-wide set of gene deletions in the fission yeast Schizosaccharomyces pombe. *Nat Biotechnol* **28**, 617-23 (2010).
15. Marguerat, S. *et al*. Quantitative analysis of fission yeast transcriptomes and proteomes in proliferating and quiescent cells. *Cell* **151**, 671-83 (2012).
16. Ryan, C.J. *et al*. Hierarchical modularity and the evolution of genetic interactomes across species. *Mol Cell* **46**, 691-704 (2012).
17. Klambauer, G. *et al*. cn.MOPS: mixture of Poissons for discovering copy number variations in next-generation sequencing data with a low false discovery rate. *Nucleic Acids Res* **40**, e69 (2012).

18. Layer, R.M., Chiang, C., Quinlan, A.R. & Hall, I.M. LUMPY: a probabilistic framework for structural variant discovery. *Genome Biol* **15**, R84 (2014).
19. Rausch, T. *et al*. DELLY: structural variant discovery by integrated paired-end and split-read analysis. *Bioinformatics* **28**, i333-i339 (2012).
20. Ye, K., Schulz, M.H., Long, Q., Apweiler, R. & Ning, Z. Pindel: a pattern growth approach to detect break points of large deletions and medium sized insertions from paired-end short reads. *Bioinformatics* **25**, 2865-71 (2009).
21. Bitton, D.A. *et al*. AnGeLi: A Tool for the Analysis of Gene Lists from Fission Yeast. *Front Genet* **6**, 330 (2015).
22. Chikashige, Y. *et al*. Gene expression and distribution of Swi6 in partial aneuploids of the fission yeast Schizosaccharomyces pombe. *Cell Struct Funct* **32**, 149-61 (2007).
23. Dobzhansky, T. On the Sterility of the Interracial Hybrids in Drosophila Pseudoobscura. *Proc Natl Acad Sci U S A* **19**, 397-403 (1933).
24. Muller, H.J. Reversibility in Evolution Considered from the Standpoint of Genetics. *Biological Reviews* **14**, 261–280 (1939).
25. Delneri, D. *et al*. Engineering evolution to study speciation in yeasts. *Nature* **422**, 68-72 (2003).
26. Noor, M.A., Grams, K.L., Bertucci, L.A. & Reiland, J. Chromosomal inversions and the reproductive isolation of species. *Proc Natl Acad Sci U S A* **98**, 12084-8 (2001).
27. Carr, A.M., MacNeill, S.A., Hayles, J. & Nurse, P. Molecular cloning and sequence analysis of mutant alleles of the fission yeast cdc2 protein kinase gene: implications for cdc2+ protein structure and function. *Mol Gen Genet* **218**, 41-9 (1989).
28. Dunham, M.J. *et al*. Characteristic genome rearrangements in experimental evolution of Saccharomyces cerevisiae. *Proc Natl Acad Sci U S A* **99**, 16144-9 (2002).
29. Itsara, A. *et al*. De novo rates and selection of large copy number variation. *Genome Res* **20**, 1469-81 (2010).
30. Zhang, F., Gu, W., Hurles, M.E. & Lupski, J.R. Copy number variation in human health, disease, and evolution. *Annu Rev Genomics Hum Genet* **10**, 451-81 (2009).
31. Stranger, B.E. *et al*. Relative impact of nucleotide and copy number variation on gene expression phenotypes. *Science* **315**, 848-53 (2007).
32. Sudmant, P.H. *et al*. An integrated map of structural variation in 2,504 human genomes. *Nature* **526**, 75-81 (2015).
33. Holtgrewe, M. Mason-A Read Simulator for Second Generation Sequencing Data. (Institut für Mathematik und Informatik, Freie Universität Berlin, 2010).
34. Danecek, P. *et al*. The variant call format and VCFtools. *Bioinformatics* **27**, 2156-8 (2011).

35. Sedlazeck, F.J., Rescheneder, P. & von Haeseler, A. NextGenMap: fast and accurate read mapping in highly polymorphic genomes. *Bioinformatics* **29**, 2790-1 (2013).
36. Faust, G.G. & Hall, I.M. YAHA: fast and flexible long-read alignment with optimal breakpoint detection. *Bioinformatics* **28**, 2417-24 (2012).
37. Li, H. *et al*. The Sequence Alignment/Map format and SAMtools. *Bioinformatics* **25**, 2078-9 (2009).
38. Thorvaldsdottir, H., Robinson, J.T. & Mesirov, J.P. Integrative Genomics Viewer (IGV): high-performance genomics data visualization and exploration. *Brief Bioinform* **14**, 178-92 (2013).
39. Untergasser, A. *et al*. Primer3--new capabilities and interfaces. *Nucleic Acids Res* **40**, e115 (2012).
40. Lenglez, S., Hermand, D. & Decottignies, A. Genome-wide mapping of nuclear mitochondrial DNA sequences links DNA replication origins to chromosomal double-strand break formation in Schizosaccharomyces pombe. *Genome Res* **20**, 1250-61 (2010).
41. Lyne, R. *et al*. Whole-genome microarrays of fission yeast: characteristics, accuracy, reproducibility, and processing of array data. *BMC Genomics* **4**, 27 (2003).
42. Drummond, A.J., Suchard, M.A., Xie, D. & Rambaut, A. Bayesian phylogenetics with BEAUti and the BEAST 1.7. *Mol Biol Evol* **29**, 1969-73 (2012).
43. DePristo, M.A. *et al*. A framework for variation discovery and genotyping using next-generation DNA sequencing data. *Nat Genet* **43**, 491-8 (2011).
44. Garrison, E. & Marth, G. Haplotype-based variant detection from short-read sequencing. *arXiv preprint arXiv* **1207.3907** (2012).
45. Speed, D., Hemani, G., Johnson, M.R. & Balding, D.J. Improved heritability estimation from genome-wide SNPs. *Am J Hum Genet* **91**, 1011-21 (2012).
46. Benito, A. *et al*. Selected Schizosaccharomyces pombe Strains Have Characteristics That Are Beneficial for Winemaking. *PLoS One* **11**, e0151102 (2016).

Acknowledgments

We thank Günter Klambauer for advice on cn.MOPS and Michael C. Schatz for helpful discussions and comments on the manuscript. F.S. was supported through National Science Foundation awards (DBI-1350041) and National Institutes of Health award (R01-HG006677). D.J., M.H., C.R. were supported by a Wellcome Trust Senior Investigator Award to J.B. (grant 095598/Z/11/Z). J.B. was supported by a Royal Society Wolfson Research Merit Award.

Author contributions

DJ, FS, CD and JB conceived and developed the study. DJ, CJ and FS conducted the bioinformatics analysis. DJ designed the laboratory work. FS designed and implemented SURVIVOR. DS contributed to analysis of heritability and GWAS. CR and MH produced the expression array analysis. MH conducted PCR validation of variants. JB provided the majority of funding for personnel and research costs. DJ, FS, CJ, CD and JB wrote the manuscript.

Supplementary Figures

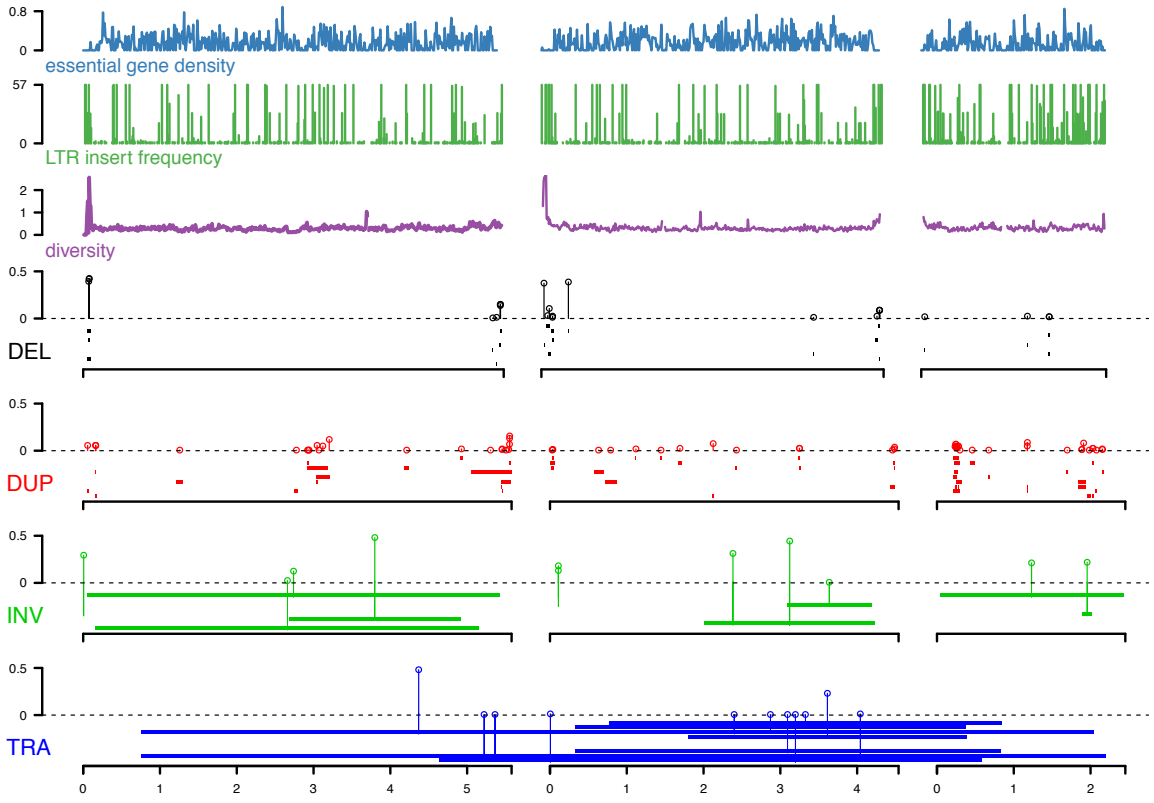

Supplementary Figure 1. Locations and minor allele frequencies of all structural variants in curated data set. Each of the three chromosomes is indicated by black bar, with scale (in megabases) at bottom. From top (same data as Fig 1): density of essential genes (blue), locations of *Tf*-type retrotransposons (green), and diversity (π, average pairwise diversity from SNPs, purple). Bar heights for deletions and duplications are proportional to minor allele frequency, the scale for retrotransposons is the frequency of the insertion in the 57 non-clonal strains. Diversity and retrotransposon were calculated from 57 non-clonal strains as described in Jeffares, et al. [10]. Below, we show different types of SVs: deletions (black), duplications (red), inversions (green) and translocations (blue). The vertical lines terminating with open circles above dotted lines emit from the mid-point of each SV and indicate the minor allele frequencies in the population of 161 strains.

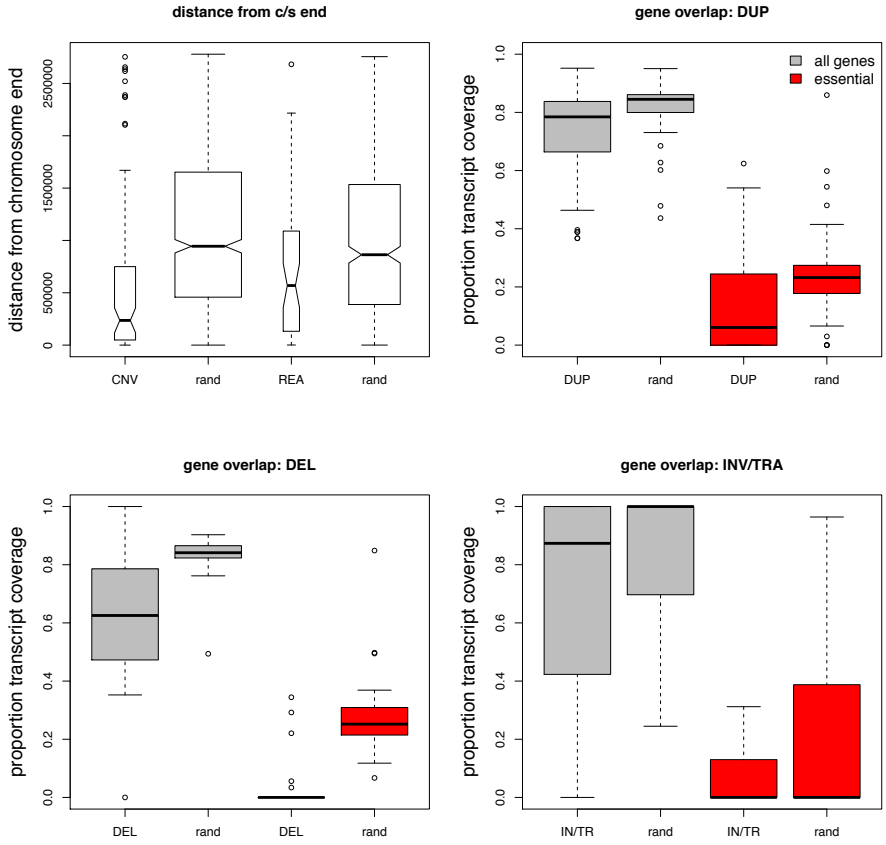

Supplementary Figure 2. Structural variations are biased towards chromosome ends and to low gene density regions. Top left panel, both CNVs and rearrangements (REA) are closer to the nearest chromosome end than the null distribution (rand), (Wilcoxon rank sum test, P-values 1.3×10^{-11} and 0.03, respectively). All other panels, calculated proportion of each duplication and deletion that contained all protein-coding or essential genes. Box plots show the distributions of these proportions for all genes (grey), and proportion of coverage by essential genes (red), compared to the null distribution (rand). All comparisons were significantly less than the null distributions (Wilcoxon rank sum test, P-values $< 1.6 \times 10^{-4}$). The same analysis was performed with the junctions of inversions and translocations, by calculating the transcript coverage in the region 500 bp up- and down-stream of the predicted start and end junctions. These rearrangements are slightly biased away from genes ($P = 1.9 \times 10^{-3}$), but not significantly biased away from essential genes ($P > 0.05$). The null distributions were determined by selecting 10 regions for each actual variant/junction that were the same size, and were placed in random positions on the same chromosome and calculating the gene coverage of these regions. Essential genes were those with the Fission Yeast Phenotype Ontology term defined as FYPO:0002061 ("inviable") in PomBase.

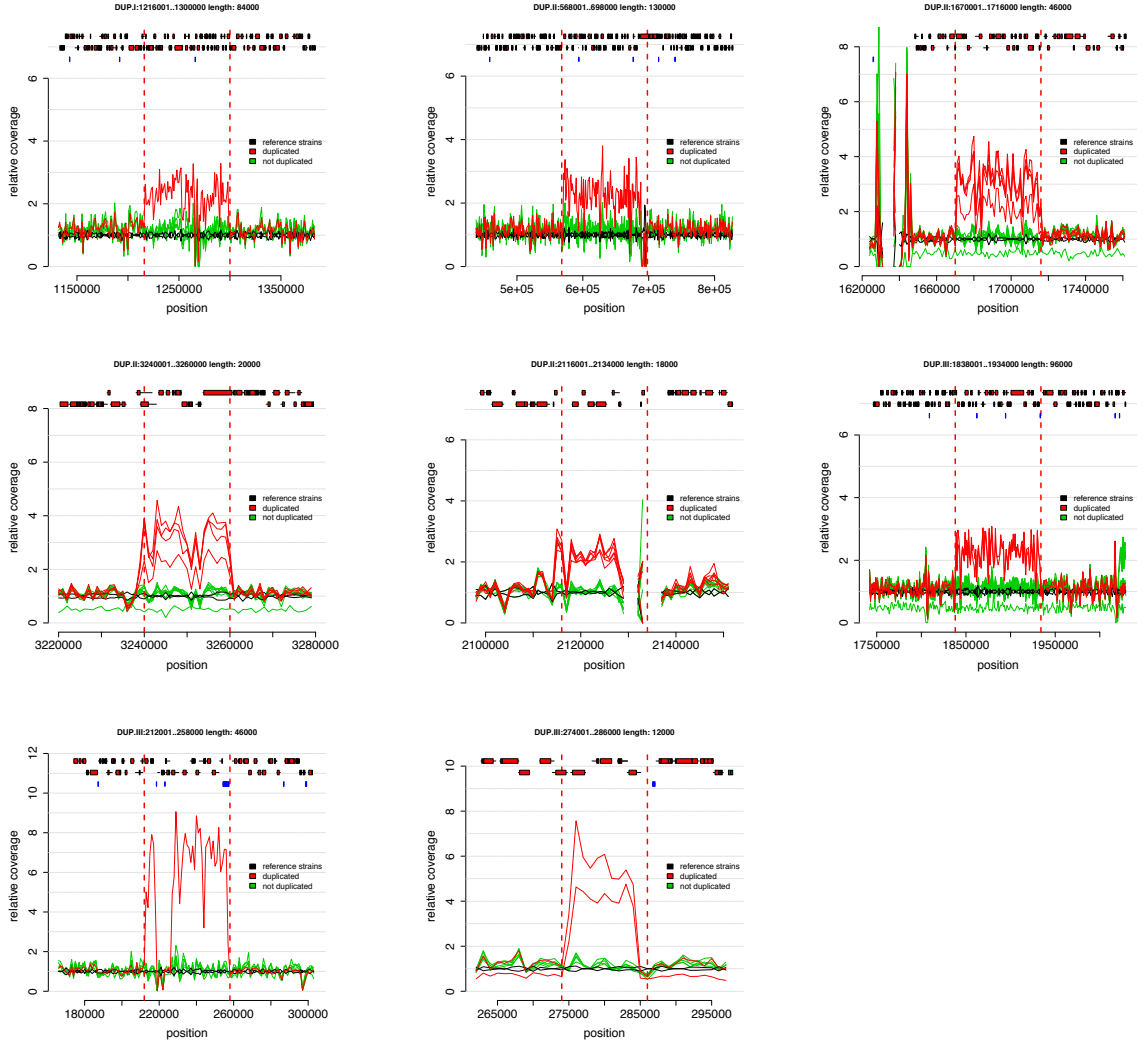

Supplementary Figure 3. Duplications that segregate within closely related strains. Plots show the average coverage in 1 kb non-overlapping windows for strains with a duplication (red) and all closely related strains without duplication (green); all these strains differ by <150 SNPs. The coverage of the two standard reference strains (h^+ and h^-) is shown in black. Top row, from left: variant DUP.I:1216001..1300000 (cluster 12, from Japan in 57), DUP.II:568001..698000 (cluster 12), DUP.II:1670001..1716000 (cluster 2, unknown origin), second row DUP.II:3240001..3260000 (cluster 2), DUP.II:2116001..2134000 (cluster 1, includes reference strain from French grapes in 1947), DUP.III:1838001..1934000 (cluster 2, various locations 1921-22). Bottom row: DUP.III:212001..258000 (cluster 6, Jamaica/USA), and DUP.III:274001..286000 (cluster 5, Sicily 1966). Genes are shown on top of plots with exons as red rectangles and retrotransposon LTRs as blue rectangles.

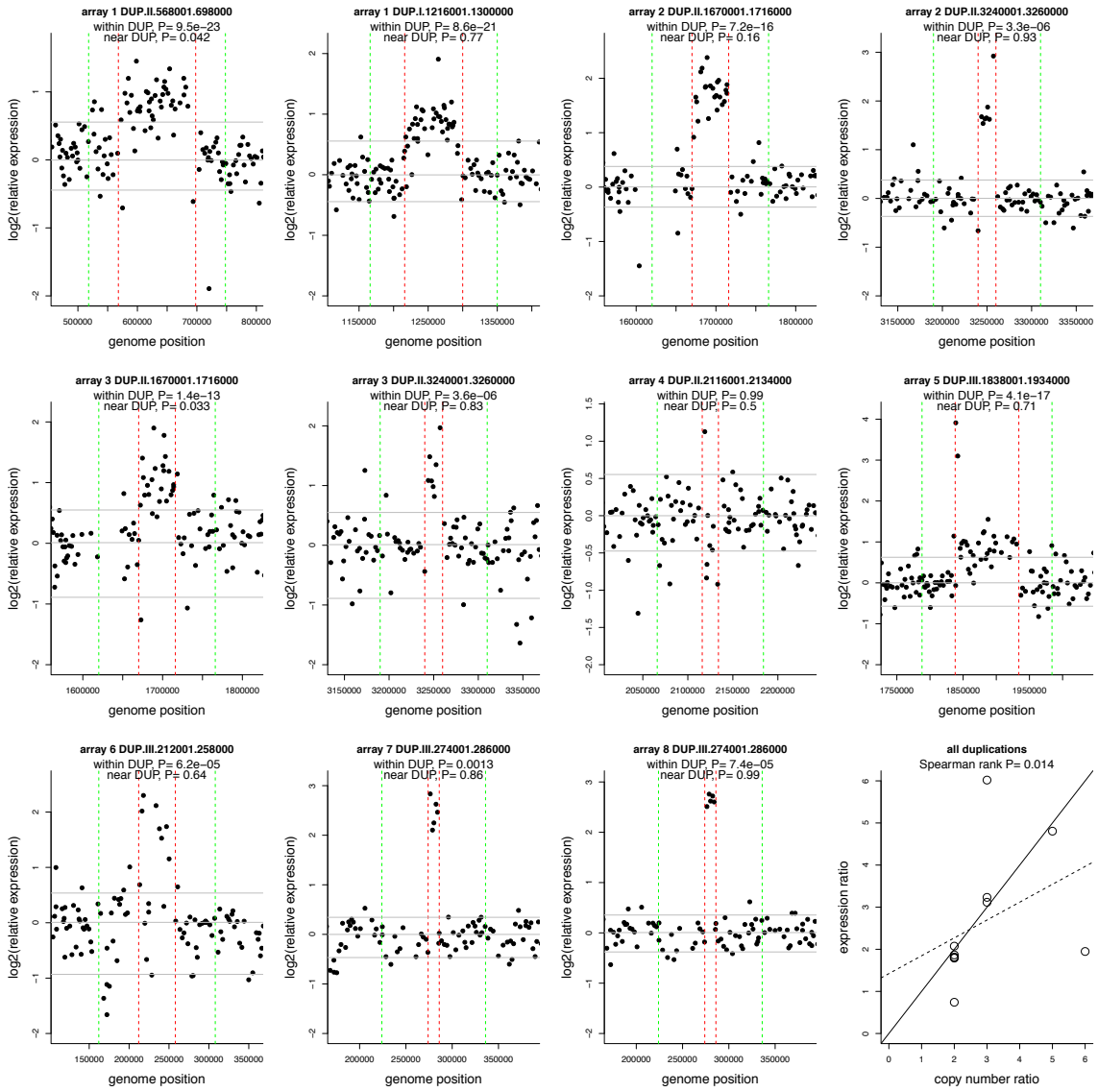

Supplementary Figure 4. No significant increase in gene expression immediately adjacent to duplications. For each duplication examined with DNA arrays, we show the relative expression (strain 1 *vs* strain 2) near the duplication. P-values show the support for the genes within the duplication (red vertical lines), or the 50 kb adjacent to the duplication (green vertical lines) being more highly expressed than all other genes in the chromosome (one-sided Wilcoxon rank sum tests). The grey horizontal lines show the 5th, 50th and 95th percentiles for gene expression data on the chromosome. The bottom right panel shows that the median increase in expression level within a duplication correlates with the increase in genomic copy number. The solid back line shows the expected increase for the 1:1 correspondence between genomic copy number and relative expression (the line $y=x$), and the dashed line shows the linear model for the data.

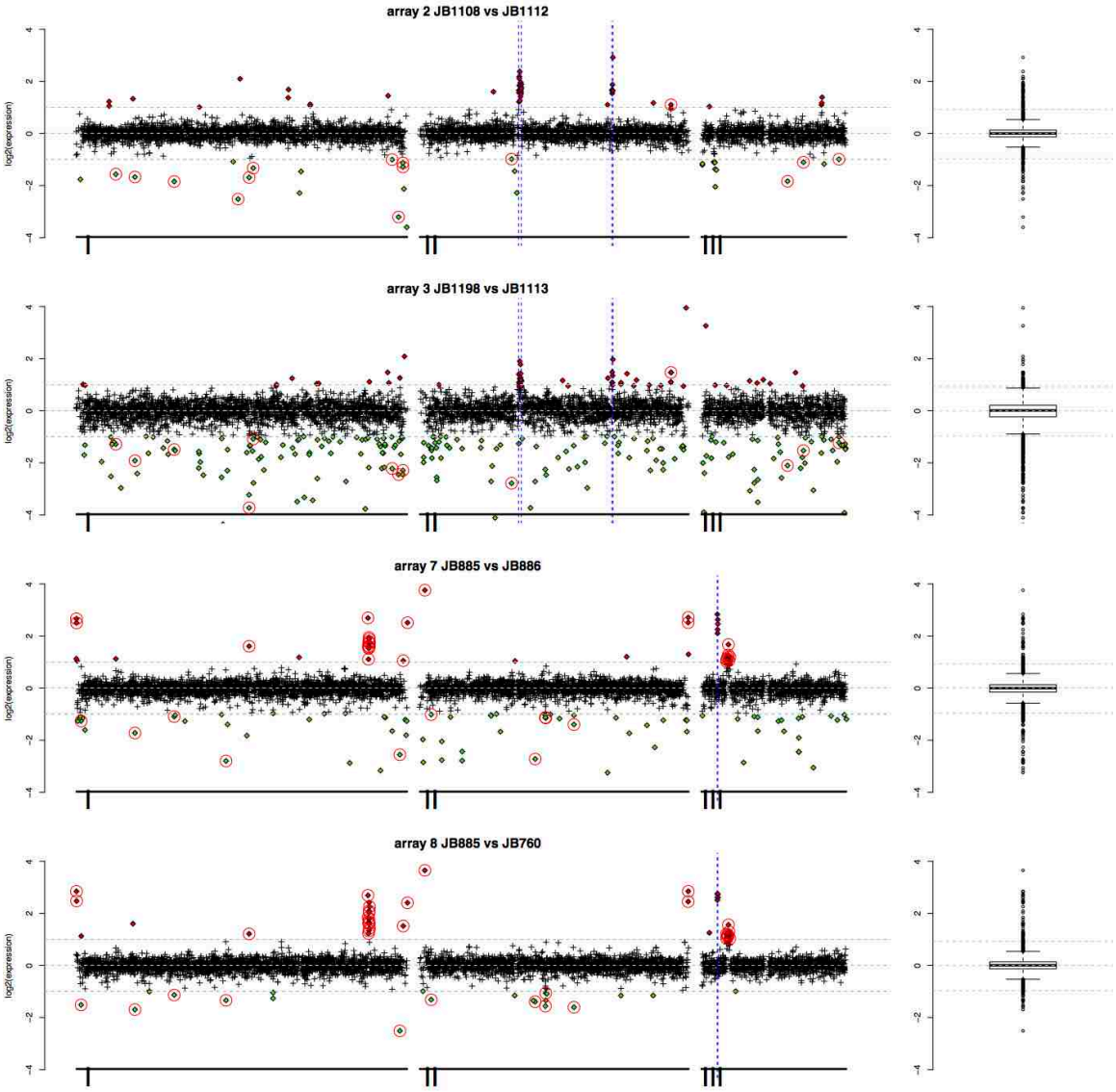

Supplementary Figure 5. Chromosome-scale view of gene expression changes. The relative gene expression levels (strain1/strain2) for arrays 2 and 3, and arrays 7 and 8 are shown with their positions on the three chromosomes. Filled circles indicates genes that we consider to be upregulated (red) or repressed (green). Those highlighted with open red circles are consistently altered in both arrays (either 2+3, or 7+8). The blue lines show where the segregating duplications are. Box plots at right show the spread of data.

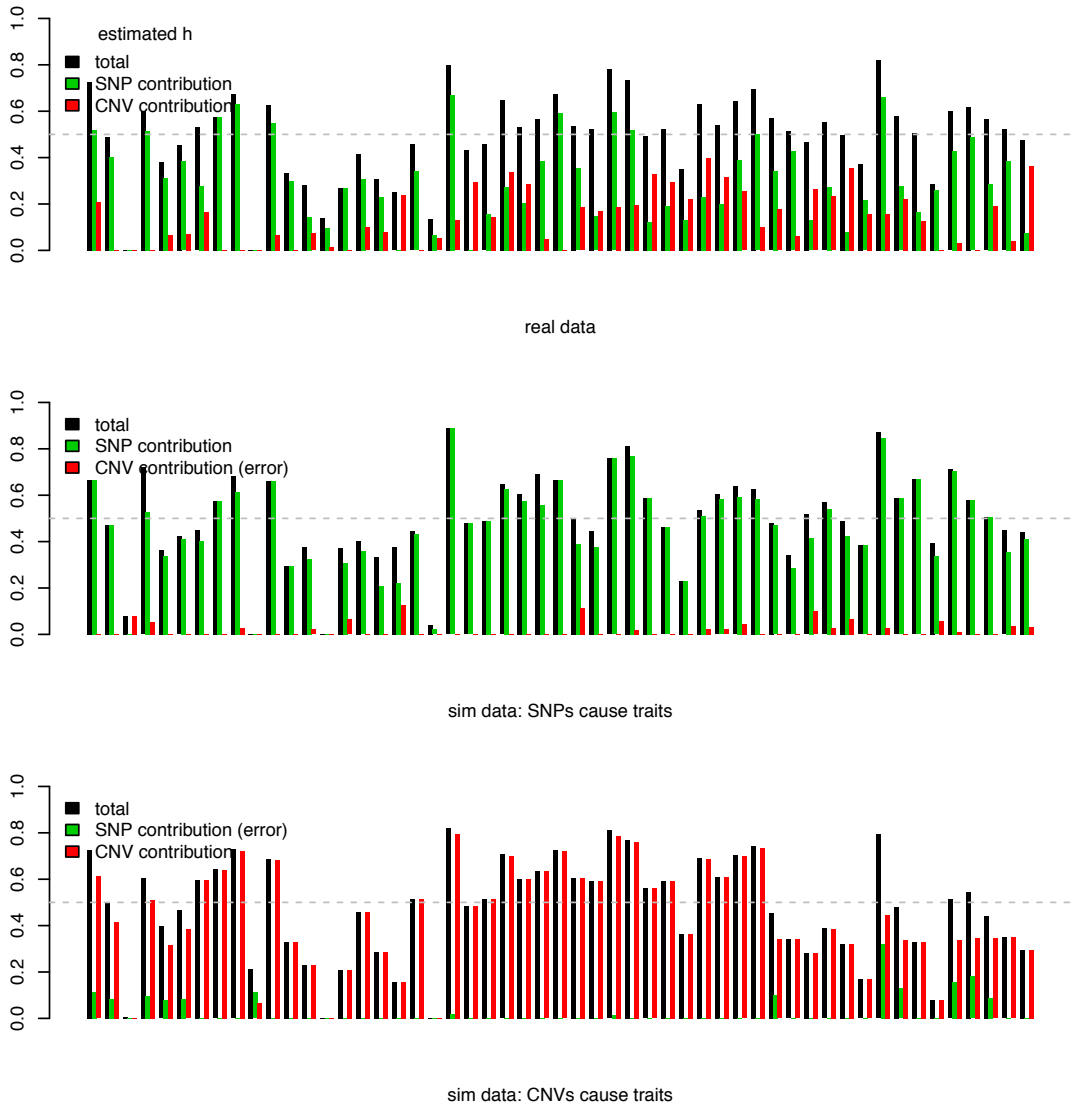

Supplementary Figure 6. Contributions of SNPs and CNVs to traits. Top panel: for 53 traits, we show the total heritability estimated by the combination of 243,289 SNPs, 87 CNVs and 26 rearrangements (grey bars). The estimates for the contributions of SNPs (green) and CNVs (red) are also shown. We then simulated data that was entirely due to the effects of SNPs (middle panel), or entirely due to the effects of CNVs (lower panel). In the middle panel, all estimates of the, usually minor, contribution of CNVs is artefactual. In the lower panel all estimates of the contribution of SNPs is artefactual. Again, these estimated are usually minor.

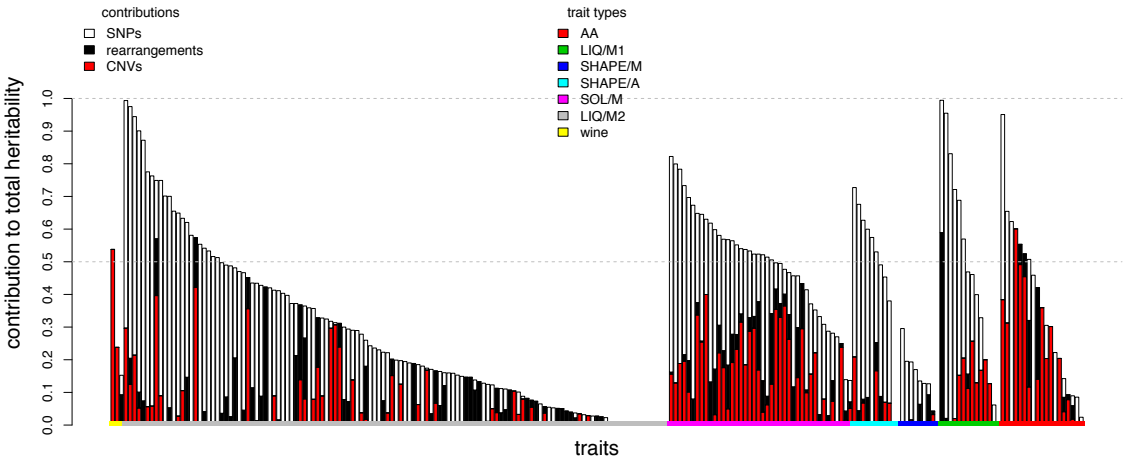

Supplementary Figure 7. Contributions to of CNVs, rearrangements and SNPs to quantitative traits. For 223 traits we show the contribution of CNVs (red), rearrangements (black) and SNPs (open bars) to the heritability. Traits are sorted by trait type (indicated by coloured bars on *x* axis), and then by total heritability estimate. Categories are wine traits (yellow), growth on liquid media (LIQ/M2; black), growth on solid media (SOL/M; magenta), automated shape parameters (SHAPE/A; cyan), manual parameters (SHAPE/M; blue), growth on liquid media from this study (LIQ/M1; green) and amino acid concentrations (AA; red). All traits are from[10], except LIQ/M2[5] and wine[46].

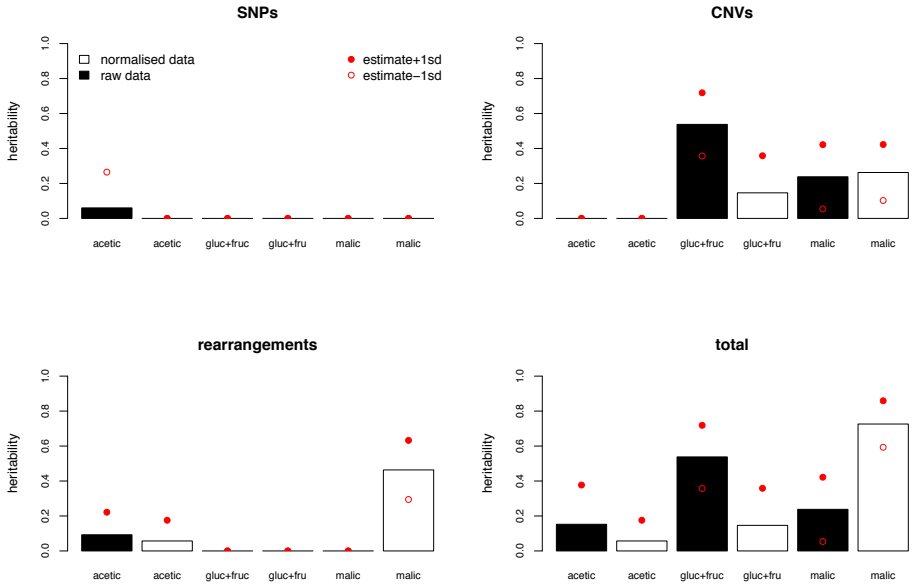

Supplementary Figure 8. Details of the heritability of winemaking traits. Previously, we examined the potential of the 57 non-clonal strains for winemaking[46]. Three parameters of fermentations in grape must, that are known to influence wine quality, were measured for all strains; the acetic acid content (acetic), the residual glucose + fructose concentration (gluc+fruc), and the percentage of malic acid degradation (malic). Bar plots show the estimated contribution of SNPs, CNVs and rearrangements to these traits, using both normalized and raw (non-normalized) data. The final plot shows the total heritability. Filled red circles show one standard deviation above the estimate, open red circles show one standard deviation below. While estimates vary with normalized/raw data, the SNP contributions are always low compared to SVs, and are not significantly greater than zero for residual glucose + fructose concentration and malic acid degradation.

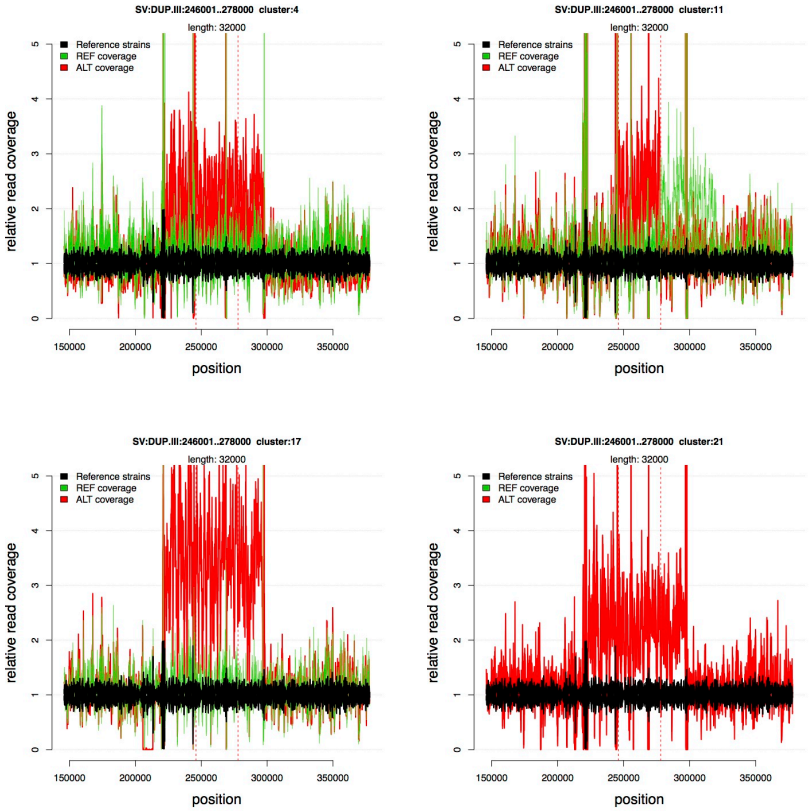

Supplementary Figure 9. The 32kb duplication associated with resistance to Brefeldin. Panels show relative coverage in 100bp windows (vs. reference genome) for strains within clonal populations ('clonal clusters'). The coverage for strains that contain the duplication are plotted in red, and those that do not are plotted in green. Reference strain coverage (h^- and h^+) is shown in black. The red vertical dashed line indicates the boundaries of the 32kb duplication – note that some clusters contain a larger duplicated region. Clockwise from top left we show clusters 4, 11, 17 and 21 (see **Supplementary Table 7** for cluster members).

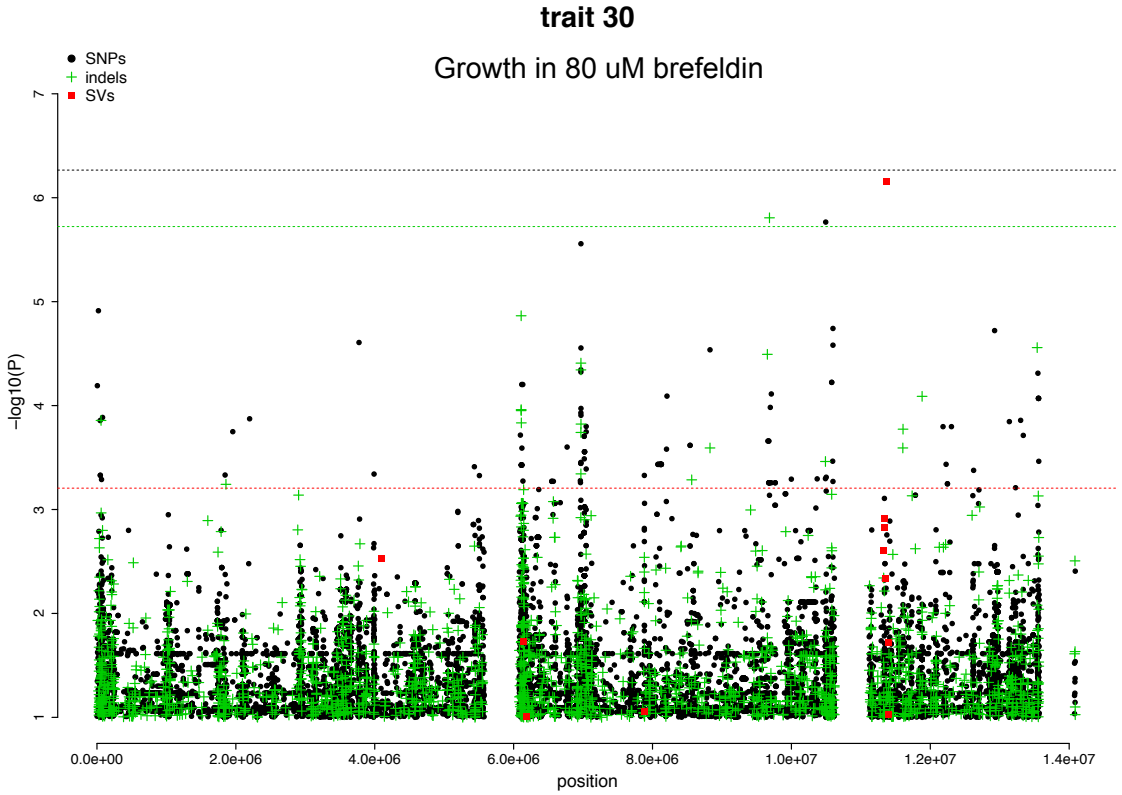

Supplementary Figure 10. Manhattan plot for all variants vs. resistance to Brefeldin. Only variants with association P-values <0.1 are shown, including SNPs (black filled circles), indels (green crosses), and SVs (red squares). Variants from the three chromosomes are shown, from left to right, followed by variants from the mitochondrial genome. The 32 kb duplication on chromosome III is the most significant variant. The horizontal dashed lines show the significance threshold derived from 1000 permutations for SNPs (black), indels (green) and SVs (red). Each is set to ensure a 5% family-wise error rate. The trait measured in this case was colony size in the presence of 80 μM Brefeldin (as a ratio of colony size without Brefeldin). Similar results, including a significant P-value for the 32kb duplication were found with 40 μM and 120 μM Brefeldin (**Supplementary Table 8**).

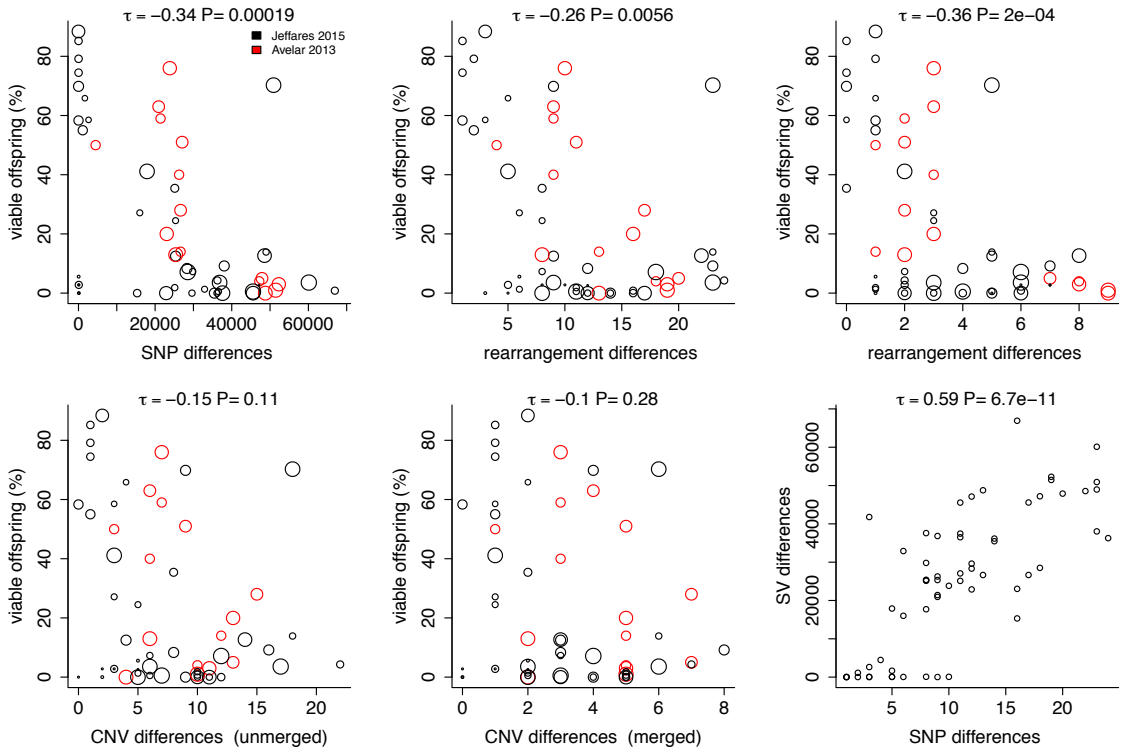

Supplementary Figure 11. Correlations between spore viability, parental SNP-genetic distance and parental SV-genetic distance. Spore viability was measured for 58 crosses in total, including data from both Jeffares, et al. [10] (black) and Avelar, et al. [4] (red), with each circle representing one cross. Unmerged CNV differences count any CNV as being different between parents when either start or end coordinates are more than 1 kb apart. Because this definition can cause us to count largely overlapping events as 'different', we also counted 'merged' differences where two CNVs were considered different only if their overlap was >50% of the total of both variants. This approach will exclude nested CNVs. CNV-genetic distance is not significantly correlated with viability in either case.

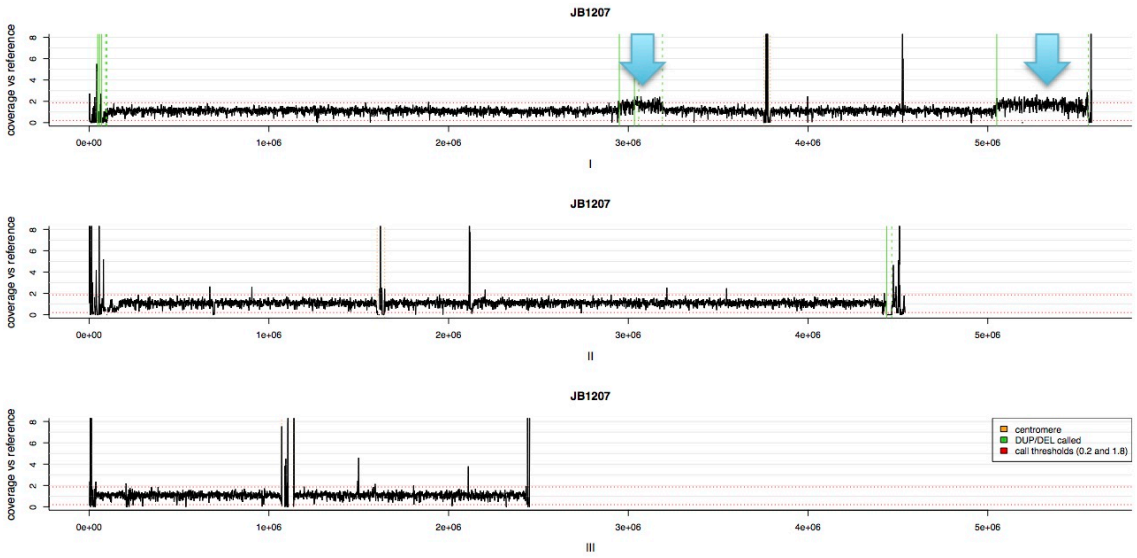

Supplementary Figure 12. Chromosome-scale read coverage plots for three chromosomes of strain JB1207. Coverage is calculated relative to the reference strain (JB22 in our collection). Two large duplications that did not satisfy the criteria used to detect CNVs with cn.MOPs are indicated with blue arrows (DUP.I:2950001..3190000, 240kb and DUP.I:5050001..5560000, 510kb).